



19

Abstract

20 The study applies the improved cloud-free Moderate Resolution Imaging Spectral radiometer
21 (MODIS) daily snow cover product (MODMYD_MC) to investigate the snow cover variations
22 from snow Hydrologic Year (HY) HY2000 to HY2013 in the Amur River Basin (ARB), northeast
23 Asia. The fractions of forest cover were 38%, 63% and 47% in 2009 in China (the southern ARB),
24 Russia (the northern ARB) and ARB, respectively. Forest demonstrates complex influences on the
25 snow accumulation and melting processes and on optical satellite snow cover mapping. Validation
26 results show that MODMYD_MC has a snow agreement of 88% against *in situ* snow depth (SD)
27 observations ($SD \geq 4\text{cm}$). The agreement is about 10% lower at the forested stations than at the
28 non-forested stations. Snow Cover Durations (SCD) from MODMYD_MC are 20 days shorter than
29 ground observations ($SD \geq 1\text{cm}$) at the forested stations, while they are just 8 days shorter than
30 ground observations ($SD \geq 1\text{cm}$) at the non-forested stations. Annual mean SCDs in the forested
31 areas are 21 days shorter than those in the nearby farmland in the SanJiang Plain. SCD and Snow
32 Cover Fraction (SCF) are negatively correlated with air temperature in ARB, especially in the snow
33 melting season, when the mean air temperature in March and April can explain 86% and 74% of the
34 mean SCF variations in China and Russia, respectively. From 1961 to 2015, the annual mean air
35 temperature presented an increase trend by $0.33^\circ\text{C}/\text{decade}$ in both China and Russia, while it had a
36 decrease trend during the study period from HY2000 to HY2013. The decrease of air temperature
37 resulted in an increase of snow cover although the increase of snow cover was not significant above
38 the 90% confidence level. SCD and SCF had larger increase rates in China than in Russia, and they
39 were larger in the forested area than in the nearby farmland in similarly climatic settings in the
40 SanJiang Plain. The air temperature began to increase again in 2014 and 2015, and the increasing
41 air temperature in ARB projects a decrease of snow cover extent and periods in the coming years.

42 **Keywords: MODIS; Snow cover; Increasing; Amur River Basin;**



43 1. Introduction

44 Seasonal snow covers about 45% of the Northern Hemisphere land areas in winter, e.g., 46%
45 and 47% in January of 2014 and 2015, respectively (Robinson, 2015). Mean monthly snow-cover
46 extent in the Northern Hemisphere has declined at a rate of 1.3% per decade over the last 40 years,
47 and most decrease occurred in spring and early summer (Barry et al., 2009). In March and April, the
48 mean snow cover extent in Northern Hemisphere decreased $1.6\% \pm 0.8\%$ per decade in the period
49 from 1967 to 2012 (IPCC, 2013). Snow cover variations in the spring season have critical
50 consequences for surface energy and water budgets and significant implications for cold region
51 ecosystems (Yang et al., 2003; Chapin et al., 2005; Brown et al., 2007). The projected continuing
52 increase of air temperature also suggests more snow cover reduction for mid latitudes by the end of
53 this century (IPCC, 2013). Reduction of snow cover extent acts as a positive feedback to global
54 warming by reducing the land surface albedo, and also affects the structure of ecosystem due to the
55 interactions of plants and animals with snow (Barry et al., 2009).

56 The Amur River forms a large part of the border between Russia and China, and near half of the
57 Amur River Basin (ARB) is within the Heilongjiang, Inner Mongolia and Jilin Provinces of China.
58 This region is one of the three primary snow distribution centers in China. About one fifth of water
59 resources in ARB are attributed to snowfall, and most areas are covered by snow over four months
60 each year (Chen et al., 2014; Wang et al., 2014). According to the land cover product of
61 MCD12Q1 in 2009 (Friedl et al., 2010), forest was about 47% in ARB and has a complex influence
62 on snowpack duration (Varhola et al., 2010; Dickerson-Lange et al., 2015; Moeser et al., 2016). In
63 the past half century, more and more wetland and forest had been drained and converted to farmland
64 in the Sanjiang Plain between Ussuri River and Songhua River (main tributaries of the Amur River)



65 in the Heilongjiang Province, China (Wang et al., 2006; Xu et al., 2012). The cultivated land area
66 increased from 7, 900 km² to 52, 100 km², and population density increased from 13 to 78 persons
67 per km² from 1949 and 2000; in contrast, the wetlands decreased from 53, 400 km² to 9, 070 km²
68 during the same period (Li et al., 2004; Wang et al., 2009a). The increase in agricultural land and
69 population brought about severe pressure on the local ecosystem, such as climate and water
70 regulation, support of habitats, and food provisions (Dale and Polasky, 2007; Wang et al., 2015).

71 Several studies investigated the snow cover variations in Northeast China based on the satellite
72 snow cover products (Zhang, 2010; Lei et al., 2011; Chen et al., 2014; Wang et al., 2014), but few
73 studies examined the snow cover variations covering the entire ARB or compared the snow cover
74 variations in the forested and non-forested areas. Lei et al. (2011) evaluated the snow classification
75 accuracy of the Moderate Resolution Imaging Spectral radiometer (MODIS) 8-day standard snow
76 cover products and the Advanced Microwave Scanning Radiometer-EOS (AMSR-E) snow water
77 equivalent (SWE) in the Heilongjiang Province during 2002-2007. Zhang (2010) directly used the
78 daily MODIS Terra snow cover product to compute the snow-covered days in Northeast China by
79 only counting the snow-covered pixels under clear sky, and omitted the snow-covered pixels
80 blocked by cloud. Chen et al. (2014) analyzed the spatiotemporal variations of snow in Northeast
81 China by using the multiday combinations of MODIS snow cover products, which have a mean
82 cloud cover of 4% and mean combination period of 7 days, similar to the MODIS standard 8-day
83 maximum combination product. Cloud is one of the major factors influencing the MODIS snow
84 cover mapping, leading to underestimate the snow-covered areas. Several methods have been
85 developed to reduce or remove the cloud cover in the MODIS snow cover products (Parajka and
86 Bloschl, 2008; Liang et al., 2008b; Xie et al., 2009; Hall et al., 2010; Parajka et al., 2010; Paudel



87 and Andersen, 2011; Wang et al., 2014). Based on previous approaches, Wang et al. (2014)
88 developed an algorithm to generate a daily cloud-free snow cover product from MODIS Terra and
89 Aqua standard daily snow cover products and tested it in the Central Heilongjiang Province, China.
90 This cloud-free snow cover product provides better representation of timely snow cover variations
91 in the tested areas than previous studies in this region (Zhang, 2010; Lei et al., 2011; Chen et al.,
92 2014; Wang et al., 2014). The daily cloud-free snow cover product and the accordingly derived
93 snow maps provide critical information for snow disaster prevention and mitigation, agriculture and
94 water resources management, and are key inputs for hydrologic and climatic models as well (Wang
95 et al., 2014).

96 Therefore, the primary objectives of this study are to 1) validate the MODIS daily cloud-free
97 snow cover product developed by Wang et al (2014) using more snow depth measurements in the
98 entire Heilongjiang Province, China; and 2) apply this cloud-free snow cover product to study the
99 spatiotemporal variations of the snow cover extent in the entire Amur River Basin, especially
100 comparing the snow cover variations between the Northern ARB (Russian part) and the southern
101 ARB (China Part), and evaluating the influence of forest on snow cover mapping and variations.
102 The rest of this paper is followed by a brief description of the study area, statement on primary data
103 and methodology, presentation of results, summary and discussions.

104

105 **2. Study area**

106 The Amur River (Called HeiLongJiang in China) Basin (ARB) is located in Northeast Asia
107 ($42^{\circ}\sim 57^{\circ}$ N, $108^{\circ}\sim 141^{\circ}$ E) crossing China, Russia and Mongolia, with a total area of 2.08×10^6
108 km^2 (Fig.1). The southern portion of ARB is located in China (43% of the ARB area), the northern



109 and eastern part is in Russia (49%), and only a small part in the southwestern upstream is in
110 Mongolia (9%). The Amur River originates in the mountains of Great Hingans in China and the
111 Cherskogo in Russia, firstly flows towards northeast, then slowly turns to southeast in a great arc
112 after the upstream Shilka River and Argun River meet together, and finally changes back towards
113 northeast and pours into the Strait of Tartary, the Sea of Okhotsk. The Songhua River and Ussuri
114 River in the south are the two primary tributaries of Amur River in China, forming the Song-Liao
115 Plain and the Sanjiang Plain, respectively. Elevations in most areas are lower than 500 m and
116 partially rise up to 2500 m in the northern and eastern mountain peaks. Forests were 47% in ARB,
117 38% in China and 63% in Russia in 2009, and mainly distributes in the northern ARB and in
118 mountains. Grassland is mainly in Mongolia and China (Fig. 1). In the past half century, a large part
119 of wetlands had been converted into farmland in the Sanjiang Plain in China, which provides great
120 amount of wheat, corn, rice, green bean, etc. (Li et al., 2004). Two areas (around 3500km² each) of
121 farmland and forest in the Sanjiang Plain are arbitrarily selected to illustrate the snow cover
122 variations (Polygons A and B in Fig. 1).

123 The climate of ARB is controlled by the high latitude East Asian monsoon, the Siberian cold,
124 dry winds from west in winter and the warm, humid ocean winds from east in summer. The annual
125 mean air temperature and precipitation in the upstream, middle stream and downstream are around
126 -2°C, 1°C, and 0°C, and 400mm, 600mm and 650mm, respectively (Yu et al., 2013). The freezing
127 days with mean air temperature below 0 °C is about 150 days per year in most areas, and it is up to
128 210 days in the northern mountains and in the Great Hinggan Mountains. Observed snow depth
129 were over 1 m in some regions. Snow covered durations in most stations in the Heilongjiang
130 Province in China ranges from 80-120 days per year, and even longer than 160 day at several
131 stations (Yu et al., 2013).



132 3. Data and Methodology

133 3.1 Snow depth and air temperature

134 Meteorological data are collected at 83 national standard weather stations in Heilongjiang
135 Province, China, including snow depth, precipitation and air temperature from 2000 to 2010 (Fig. 1).
136 Snow depth data are daily observations rounded to 1 cm and used to validate the MODIS snow
137 cover products. Four stations are screened out due to data quality and inconsistency, and total 79
138 stations are used for validation. In general comparison, one MODIS pixel value collocated with one
139 weather station is extracted to compare with the corresponding *in situ* snow depth data. To minimize
140 the impacts of the spatial representative error of *in situ* measurements, the snow depth data ≥ 4
141 cm are used to validate the accuracy of MODIS snow cover mapping, and other data of 0 cm (no
142 snow) and 1-3cm (patchy snow) are also provided for assistance (Parajka and Blöschl, 2008; Wang
143 et al., 2008, 2009b).

144 In a detailed investigation within snow hydrologic years (HY) from September 1, 2007 to
145 August 31, 2008 (HY2007) with minimum snow and HY2009 with maximum snow, the averages of
146 different-size pixel patches are compared with the snow depth data centered at each one of the four
147 weather stations, representing cultivated farmland (S31), natural grassland (S53) and forests (S12
148 and S52). The pixel patches consist of pixels 1×1 , 3×3 , 5×5 , 9×9 , and 21×21 pixels,
149 corresponding to areas of $0.5 \text{ km} \times 0.5 \text{ km}$, $1.5 \text{ km} \times 1.5 \text{ km}$, $2.5 \text{ km} \times 2.5 \text{ km}$, $4.5 \text{ km} \times 4.5 \text{ km}$, and
150 $10.5 \text{ km} \times 10.5 \text{ km}$.

151 Besides the snow depth data at the 83 stations in Heilongjiang Province, daily mean air
152 temperature data at 18 stations in China and 22 stations in Russia are downloaded from the Global
153 Historical Climatology Network (GHCN), <http://www.ncdc.noaa.gov/oa/climate/ghcn-daily>. Some



154 of the GHCN stations are same to part of the 83 meteorological stations (Fig. 1). The time spans
155 from 1961 to 2015 for daily air temperature.

156 **3.2 MODIS standard snow cover products**

157 Identical MODIS instruments are carried on both Terra and Aqua satellites, which were
158 launched in December 1999 and May 2002 and pass the equator at the local time of 10:30 am and
159 1:30 pm, respectively. A series of standard snow cover products are generated using the same
160 algorithm from both Terra and Aqua MODIS reflectance data (Hall et al., 2002, 2010; Wang et al.,
161 2009b). These standard products include the daily MOD10A1 (Terra) and MYD10A1 (Aqua) and
162 the 8-day maximum composite of MOD10A2 and MYD10A2 with 500m spatial resolution and 10
163 degree by 10 degree tiles, and the daily, 8-day maximum and monthly mean snow cover products of
164 MOD10C1-3 and MYD10C1-3 with 0.05° global climate model grid (Wang et al., 2014).

165 The 500-m MODIS Terra/Aqua daily MOD/MYD10A1 snow cover products from 2000 to
166 2014 are used in this study. Six MODIS tiles are required to cover the entire the Amur River Basin.
167 These tiles are h24v03, h25v03, h25v04, h26v03, h26v04 and h27v04. All MODIS data are
168 downloaded from the National Snow and Ice Data Center (NSIDC) (<http://nsidc.org/data/modis>).
169 Snow cover variations are analyzed mainly in a snow hydrological year, beginning on September 1
170 and ending on next August 31. For instance, HY2013 refers to a period from September 1 of 2013
171 to August 31 of 2014 (Wang and Xie, 2009).

172 **3.3 Improved MODIS snow cover product**

173 Cloud blockage is a severe impediment for optical satellite snow cover mapping. For examples,
174 the annual mean cloud fraction is about 50% and can be up to 95% in several continuous days in the



175 Northern Xinjiang, China and on the Colorado Plateau, U.S. (Wang et al., 2008; Xie et al., 2009).
176 Fortunately, snow cover remains relatively stable in a couple of hours and even days especially in
177 winter compared to the cloud cover. The three-hour difference that satellites Terra and
178 Aqua/MODIS pass the equator allows us to combine the morning and afternoon observations of
179 MODIS Terra/Aqua to obtain a cloud-less snow cover product (Parajka and Bloschl, 2008; Wang et
180 al., 2009b; Xie et al., 2009). The improved cloud-free MODIS daily snow cover product
181 (MODMYD_MC) is generated from the MODIS Terra/Aqua standard daily snow cover product by
182 a cloud-removal algorithm (Wang et al., 2014). This algorithm included two automated steps. Firstly,
183 the daily snow cover images of MOD10A1 and MYD10A1 are combined to generate a daily
184 maximum snow cover image called MODMYD_DC. Then, the cloud pixels on the current-day
185 MODMYD_DC (n) are replaced by the previous-day MODMYD_DC (n-1) cloud-free pixels on
186 day (n-k) until all cloud pixels are replaced, finally generating a daily cloud-free snow cover
187 product. The number of cloud-persistent days (k) k is normally less than 5 days in the tested tile of
188 h26v04 although it is not limited in the replacement (Wang et al., 2014).

189 **3.4 MODIS land cover product**

190 MODIS land cover product of MCD12Q1 in 2009 is used to classify the land cover type in
191 ARB (Friedl et al., 2010). MCD12Q1 was generated by ensemble supervised approaches with
192 various classification systems. MCD21Q1 have five land cover classifications in each calendar year.
193 The 17-class International Geosphere-Biosphere Programme (IGBP) classification is applied in this
194 study. The land cover types at each station include deciduous coniferous forest, deciduous forest,
195 shrub, grass and crops, and are reclassified into forest (coniferous forest, deciduous forest and shrub)
196 and non-forest (grass and crops). In the entire ARB, all land cover types are also classified into



197 forest and non-forest to compare the snow cover variations in the forested and non-forested areas.

198

199 **4. Results**

200 **4.1 Assessment of snow cover classification**

201 The *in situ* snow depth measurements at 79 meteorological stations are used to validate the
202 snow classification for the four MODIS snow cover products, including two daily standard products
203 (MOD10A1 and MYD10A1), one daily combination (MODMYD_DC) and one multi-day
204 combination (MODMYD_MC). Snow depth measurements are divided into three groups: snow
205 depth ≥ 4 cm (snow), $1 \text{ cm} \leq \text{snow depth} \leq 3 \text{ cm}$ (fractional snow) and snow depth = 0cm (snow-free
206 land). Fig. 2 shows the mean agreements of the four products against *in situ* snow depth (≥ 4 cm)
207 measurements during the 10 snow hydrologic years (HY2000-HY2009). The large proportion
208 (~50%) of cloud blocks the MODIS instrument to retrieve the land cover under cloud, resulting low
209 agreements of snow (34-38%) and land (64-66%) mapping for the daily Terra and Aqua MODIS
210 snow cover products. The daily combination (MODMYD_DC) of MOD10A1 and MYD10A1
211 reduces cloud by 10% and increases snow and land agreements by 5-10%. For the improved daily
212 cloud-free snow cover product MODMYD_MC, agreements of snow and land classification are 88%
213 and 92%, respectively. The land and overall agreements from all 79 stations are similar to and the
214 snow agreement is slightly lower than those from the 53 stations under the MODIS tile of h26v04 in
215 the Central Heilongjiang Province, China (Wang et al., 2014).

216 The lower value of snow agreement is likely related to the fact that there are more stations
217 within forests. Fig. 3a shows that the snow agreements at forested stations is about 10% lower than
218 those at non-forested stations for the four snow cover products although their mean snow depth at



219 the forested stations is 5 cm larger, which is because most forested stations are located in higher
220 latitude and altitudes. For the fractional snow cover ($1\text{cm} \leq \text{snow depth} < 4\text{cm}$), the agreements for
221 MOD10A1, MYD10A1, MODMYD_DC and MODMYD_MC are 20%, 12%, 23% and 59% at
222 non-forested stations, respectively (Fig.3b). Compared to the two daily standard products, the snow
223 agreement of MODMYD_MC increases by 40% for the fractional snow. Similarly, the snow
224 agreements are lower at the forested stations than at the non-forested stations.

225 Fig. 4 illustrates mean agreements of snow cover duration (SCD) in each snow hydrologic year
226 from HY2000 to HY2009 between MODMYD_MC and in situ observations at 79 individual
227 stations. The agreement is computed by equation (1).

$$228 \quad A = \left(1 - \frac{|\text{SCD}_{\text{mod}} - \text{SCD}_{\text{grd}}|}{\text{SCD}_{\text{grd}}}\right) \times 100\% \quad (1)$$

229 where A represents agreement, SCD_{grd} is snow-covered days (SCD) from ground measurements
230 with snow depth $> 1\text{cm}$, SCD_{mod} is SCD recorded by MODIS (Wang et al., 2009b, 2014).

231 Generally, SCD from MODMYD_MC agrees well ($91 \pm 6\%$) with and is 8 ± 8 days shorter
232 than ground observations at the non-forested stations. This is similar to other regions, such as
233 Northern Xinjiang (Wang et al., 2009b), Colorado Plateau (Xie et al., 2009), Pacific Northwest
234 (Gao et al., 2010). In contrast, the mean SCD agreement is $79 \pm 13\%$ and 20 ± 23 days shorter than
235 ground observations at the forested stations.

236 4.2 Representative errors

237 The above analysis shows large agreement variations of snow mapping at individual stations,
238 especially within different land covers. In order to investigate these disagreements at different
239 stations and assess the representative of a single station measurements or a single pixel value within



240 different land covers, four typical stations (Fig.1) in the same sub-region are selected for detailed
241 analysis, representing cultivated farmland (S31), natural grassland (S53) and forest (S12 and S52).
242 Figure 5 displays the daily *in situ* snow depth measurements and MODMYD_MC retrievals at the
243 selected four stations from HY2000 to HY2009. Table 1 summarizes the ground measured snow
244 depth and the according MODMYD_MC retrievals.

245 At the flat stations of farmland and grassland, MODIS (MODMYD_MC) retrievals are in good
246 agreement with the *in situ* snow depth observations (Fig.5a, b, Table 1), e.g., the Snow Cover Onset
247 Date (SCOD) and Snow Cover End Date (SCED) for the continuous winter snow-covered period
248 were consistent with ground observations, except for some transient snowfall events before SCOD
249 and after SCED. Those missed transient snowfall events were caused primarily by the persistent
250 cloud blockage that snow melts away before it turns clear (Wang et al., 2009b). This indicates that
251 winter snow unanimously covers those areas and the point measurements at the clearing
252 meteorological sites have good spatial representative. At different pixel patches from 1×1 , 3×3 , 5
253 $\times 5$, 9×9 , to 21×21 pixels (0.25, 2.25, 6.25, 20.25 to 110.25 km^2), the mean values of MODIS
254 retrievals are consistent and agree well with the ground snow depth measurements especially in the
255 snow-rich year of HY2009 (Tables 2 & 3). The higher agreements in the snow-rich year of HY2009
256 again demonstrate the importance of spatial representative of snow depth measurements in
257 validating the satellite retrievals.

258 The forested stations of S12 and S52 represent a good case and a poor case of agreements,
259 respectively. At station S12, the maximum snow depth in the snow-least (HY2007) and snow-rich
260 years (HY2009) were 14 and 39 cm, respectively. Accordingly, the agreement in HY2009 was
261 higher than that in HY2007 for the different pixel patches, especially for the fractional snow (Table



262 4). Meanwhile, the agreements did not decrease evidently with the increase of pixel patches except
263 for on December 31, 2007. Fig. 5c also shows that MODIS performed poorly for HY2001, HY2002
264 and HY2007, when there were less snow and snow depth were less than 10 cm mostly. In contrast,
265 the snow depth in each year at S52 was much less than those at S12 (Fig. 5d). MODIS failed to
266 retrieve the snow in many periods when the ground observed snow but had snow depth less than 4
267 cm (Fig. 5d). In the two years of HY2007 and HY2009, MODIS agreements even increased with
268 the increase of pixels (Table 5). This again shows that part of the disagreement is caused by the poor
269 representative of ground measurements at the point scale within forested areas. It is quite
270 challenging to accurately map the snow cover and snow depth in the forested areas
271 (Dickerson-Lange et al., 2015). For the forested areas, a larger sampling area may better represent
272 the overall snow cover conditions.

273 **4.3 Snow cover variations**

274 **4.3.1 Snow cover distributions**

275 The improved cloud-free MODIS daily snow cover product (MODMYD_MC) is used to study
276 the spatiotemporal variations of snow cover in the entire Amur River Basin. Fig. 6 presents the
277 spatial distribution of the mean snow-covered days during the 14 snow hydrologic years from
278 HY2000 to HY2013 in ARB. SCDs are classified into seven categories: shorter than 30 days, 30 to
279 60 days, 61 to 90 days, 91 to 120 days, 121 to 150 days, 151 to 180 days and longer than 180 days.
280 Overall, latitude (a proxy of available solar radiation) dominates the SCD distribution. The higher
281 the latitude, the longer the mean SCD is. For example, SCD is longer than 180 days in Northern
282 ARB but less than 60 days in the southern central ARB. Elevation is the secondary factor
283 determining SCD. Mountainous areas have longer SCD than the nearby plain. SCDs in mountains



284 of Stanovoi, Tukuringer and Bureinskiy Mountain are normally longer than 150 days, while they
285 are less than 120 days in the neighboring plains.

286 Meanwhile, the forested areas show shorter SCD than the non-forested areas with similar
287 latitude and elevation, such as in the Great Hingans and their neighboring plains (Fig. 1 and Fig. 6).
288 This shorter SCD within forest could be explained from two sides. On one hand, the snow cover
289 extent is likely underestimated by the MODIS optical remote sensing techniques, and this
290 underestimate ranges from 9% to 37% across different forest densities (Raleigh et al., 2013). On the
291 other hand, there is actually shorter SCD within forest than in the nearby farmland due to the
292 complex influence of the forest on snow accumulation, redistribution, and ablation processes
293 (Varhola et al., 2010).

294 The histogram of the mean SCD in ARB shows a near normal distribution (Fig. 7). The 14-year
295 mean SCDs range from 0 to 260 days in ARB. The primary part is between 90 and 150 days, only
296 10% is less than 60 days, and 8% is longer than 180 days. The basin-scale mean SCD is 121 days in
297 ARB. Most areas are snow covered from December to March, and part of them is from October or
298 November to April (Fig. 8). Snow normally starts to cover the basin from the north and in
299 mountains in October, and then melts away in April and early May.

300 **4.3.2 Snow cover variations**

301 Mean SCF in ARB has large inter-annual variations, and the largest SCF variation ranges
302 (max-min) are in the snow accumulation period of November (29%) and December (42%) and in
303 the snow melting months of March (53%) and April (39%) (Fig. 8). All maximum snow cover
304 extent occurred in the snow accumulation and melting months of HY2012 (Fall of 2012 and Spring
305 of 2013), while the minimum snow in the accumulation and melting periods were in HY2001 (Fall



306 of 2001) and HY2007 (Spring of 2008), respectively.

307 The detailed variations of snow cover in ARB are illustrated in three snow hydrologic years by
308 four plots, SCD anomaly (a), monthly mean SCF (b), SCOD in fall (c), and SCED in spring (d) in
309 Figs. 9. These three snow hydrologic years represent a snow-poor year in HY2001, a snow-neutral
310 year in HY2005, and a snow-rich year in HY2012 (Fig. 9-11). SCD anomalies in each year are
311 grouped into seven categories with a 30-day interval: <-60 days, -60 to -31 days, -30 to -11 days,
312 -10 to 10 days (supposed to be no change), 11- 30 days, 31-60 days, and >60 days. Red colors
313 express shorter SCD below average, and the white indicate longer SCD above average (e.g., Fig.
314 9a). SCOD and SCED are also grouped into seven categories with a half month interval, from
315 October 15th to January 1st for SCOD, and from February 15th to May 1st for SCED. Similar to Fig.
316 9a, red colors represent later SCOD and earlier SCED, i.e., shorter SCD, and the white represent
317 earlier SCOD and later SCED, leading to longer SCD (e.g., Fig. 9c & d).

318 For a snow-poor year in HY2001, SCD was below the 14-year mean in most ARB (red colors)
319 except for some small areas, e.g., in the upstream of Zeya catchment in Northern ARB (Fig. 9a).
320 Monthly mean SCF was much lower than the 14-year mean in November, December, February and
321 March (Fig. 9b). In the Northern ARB, snow began to cover the land late October 2001 and began
322 to melt in early April 2002. In contrast, snow did not begin to cover the land until late December
323 2001 and melted away in February 2002 in the Southern and Western ARB (Fig. 9c & 9d).

324 For a snow-neutral year in HY2005, SCD was around the 14-year mean (dark color) in most
325 ARB. SCD was about 15 days longer than the mean in the west, central north and the downstream
326 basin, and it was 30 days shorter than the mean in southern ARB, and even 60 days shorter than the
327 mean in the Southwestern part in Mongolia (Fig. 10a). SCF was same to the 14-year mean in each



328 month (Fig. 10b). Snow normally began to cover the northern, central and southern ARB from
329 October, November and late December, and then melted away from southern ARB to Northern ARB
330 from early February, March and late April (Fig. 10c & 10d).

331 For a snow-rich year in HY2012, SCD was above the 14-year mean in most ARB, especially in
332 the southern plains (white color) and was on the opposite of HY2001 (Figs. 9a & 11a). SCF was
333 much larger than the 14-year mean from December 2012 to April 2013 (Fig. 11b). Snow began to
334 cover the entire ARB in October and November, and only some forested areas did not cover by
335 snow until early December, e.g., in the Great Xingans (Fig. 11c). Meanwhile, snow did not begin
336 melt away until late March and April in most areas, and until early May in the northern ARB (Fig.
337 11d).

338 In summary, snow cover shows large spatial and inter-annual variations. The plains and
339 cultivated farmland show much larger inter-annual variations than the mountains and forests. The
340 combination plots of SCD, SCF, SCOD and SCED together illustrate the detailed snow cover
341 variations and are significant in snow water resource, agriculture and disaster risk management.

342 **4.3.3 Snow cover changes**

343 During the 14 snow hydrological years from HY2000 to HY2013, annual SCD and the
344 March-April mean snow cover fraction (SCF) had a similar increasing trend in ARB, Russia and
345 China (Fig. 12, Table 6). The monthly mean SCF in ARB has larger variations in March and April
346 than in other months (Fig. 8). HY2012 had the largest SCF/SCD, while HY2001 and HY2007 had
347 the smallest SCF/SCD (Fig. 12). The mean SCF in March and April of 2008 showed the smallest
348 snow cover during the 14 years. Both SCD and SCFs had large inter-annual fluctuations and a
349 slightly increasing trend. China had a larger increasing rate (slope) than Russia, and March had a



350 larger increase rate than other months in China, although they were not significant above the 90%
351 confidence level in all areas (Table 6).

352 SCF was controlled dominantly by air temperature in the melting season and negatively
353 correlated with air temperature, especially in March and April, when r^2 were 0.86 in China and 0.74
354 in Russia in the 14 years (Fig.13). The increasing SCF from HY2000 to HY2013 is further
355 supported by the decreasing air temperature recorded from meteorological stations in China and
356 Russia in the same period, although the air temperature had an increase trend from 1961 to 2015
357 (Fig. 14). The mean air temperature reached a high record in 2007 and then continuously decreased
358 till 2013, resulting in an increasing SCF especially in HY2012. It began to increase again in 2014
359 and 2015. The increasing air temperature projects a further decrease of snow cover extent and
360 periods.

361 Besides the administrative boundary between Russia and China, the snow cover variations are
362 further investigated in the forested and non-forested areas. There were shorter (mean = -12 days)
363 SCD in the forested areas than in the non-forested areas although most forested areas are located in
364 the northern part and have higher elevations than the non-forested areas in the entire ARB (Fig. 15a).
365 Snow in the forested areas starts slightly later (-4 days) and melts away earlier (8 days) than those in
366 the non-forested area. During the 14 years, SCD had a slightly increasing trend in both forested and
367 non-forested areas in the entire ARB (Fig. 15a, Table 7). The increasing SCD occurred in earlier
368 SCOD and later SCED. The change rates in the forested areas were smaller than those in the
369 non-forested areas, and only SCOD changes (advance) in the non-forested areas were significant at
370 the 90% confidence level (Table 7).

371 Moreover, there were much shorter (-21 days) SCD in the forested areas than in the



372 non-forested areas in the Sanjiang Plain (Fig. 15b). Both areas (around 3 500km²) are located in a
373 same latitude ranges and selected to compare the snow cover variations. The forested area is about
374 200-300m higher than the neighboring farmland area. During the 14 years, SCD had a slightly
375 increasing trend in both forested and non-forested areas in the Sanjiang Plain (Fig. 15b, Table 8).
376 The snow starts later (14 days) and melts earlier (-6 days) in the forested area than in the
377 non-forested area. The change rates were larger in the forested areas than in the non-forested areas,
378 although these changes are not significant above the 90% confidence level but close to the
379 significant r thresholds, especially in the forested areas (Table 8).

380

381 **5. Summary and Discussions**

382 **5.1 Effects of forest on snow**

383 **5.1.1 Representative errors of ground measurements**

384 The improved daily cloud-free MODIS snow cover shows high agreements with the ground
385 snow depth measurements (Fig.2), while the snow agreements within the 79 stations is slightly
386 lower than those at the 53 stations (Wang et al., 2014). This is because most of the excess stations
387 are located within forest. The snow agreements are about 10% lower within the forested stations
388 than at the non-forested stations (Fig.3). MODIS SCDs within the forest stations are shorter than the
389 ground observations (Fig.4b), and also have lower agreements and r values with ground
390 observations than those at the non-forested stations (Fig.4a).

391 This suggests that forest is the dominant contributions to the disagreement. The point
392 observations of snow depth at the clearing meteorological sites may not represent the areal



393 distributions of snow accumulations in the neighboring forested areas (500m for a MODIS pixel).
394 The forests shows different snow accumulation and melt dynamics compared to the clearcuts. There
395 is likely less snow accumulation in the forested ground since a large part of snowfall is intercepted
396 by the forest canopy/branches (Varhola et al., 2010). For instance, peak snow accumulations
397 increased significantly from the forest edge to the nearby clearcuts of 0.5, 1 and 2 times of the forest
398 height (Golding and Swanson, 1986). Accurate estimation of snow accumulation in forested
399 watersheds is problematic, and a single snow depth measurement cannot validate a MODIS pixel
400 with confidence, especially in forested pixels (Raleigh et al., 2013). The network of dense ground
401 sensors of temperature and snow depth observations can provide good spatial representative of
402 snow accumulations under forest canopy only at limited campaign sites (e.g., Raleigh et al., 2013;
403 Dickerson-Lange et al., 2015), while the snow depth measurements at single stations are the merely
404 available data in the ARB watershed and in other large watersheds world around as well. In the
405 common point-pixel comparison, the mean value of a larger pixel patch, instead of the
406 station-located one pixel, could be a better representative to MODIS retrievals especially within the
407 forested area in some cases (Tables 4 & 5).

408 **5.1.2 Impacts of forest on MODIS snow cover mapping**

409 Besides the ground representative errors at a single clearing forest station, MODIS snow cover
410 mapping algorithm encounters challenges in the forested areas (Xin et al., 2012). The improved
411 algorithm of MODIS binary snow cover mapping in the forest mask uses the Normalized
412 Differences of Snow Index (NDSI) and the minimum reflectance (0.1) of MODIS band 4 (545-565
413 nm, green band) (Hall et al., 1995; Klein et al., 1998). Snow-covered forests usually have a much
414 lower reflectance in the green band than pure snow. Both NDSI and the reflectance of band 4 can be



415 reduced by the existence of forest stands due to the shadow and tree-snow mixture effects, resulting
416 in less snow cover estimate (Musselman et al., 2012; Dickerson-Lange et al., 2015). This
417 underestimate can be explained from two aspects. Firstly, MODIS sensors have a $\pm 55^\circ$ wide
418 across-track scan angle, which makes the view zenith angle approach 65° at the end of the scan
419 line. The large view zenith angles reduce the capability of MODIS sensor to see the forest gaps (the
420 snow-covered ground) through the tree canopy and trunks, and these gaps are essentially detectable
421 at lower view zenith angle or near the nadir view (Liu et al., 2008).

422 Secondly, in the mid and high latitude regions like ARB, the solar elevation angles are low in
423 most of snow-covered winter months. Forest cast larger shadows and shaded areas with lower solar
424 elevation angles, resulting in lower reflectance and NDSI. Our results (not shown) demonstrates
425 that MODIS snow agreements in the forested stations in Heilongjiang Province in China are 12%
426 lower in December and January (with lower elevation angles) than in February and March (with
427 higher elevation angles), while the snow agreements are similar during both periods at the
428 non-forested stations. Snow normally persists through this period from December to March at most
429 stations. As a consequence, MODIS snow cover mapping accuracy is lower in the forested areas
430 than in the non-forested areas (Hall et al., 2002; Xin et al., 2012; Raleigh et al., 2013). This again
431 illustrates the challenges in accurately mapping snow cover extent in the forested areas using
432 MODIS and other optical remote sensors. MODIS-retrieved snow extent is the best available snow
433 cover product in the forested areas at the regional and global scales with relative long-term and
434 consistent observations. The improved MODIS daily cloud-free snow cover product could present
435 the overall snow cover extent within forested areas although there is a large uncertainty.

436 **5.1.3 Effects of forest on snow accumulation and ablation**



437 SCD was shorter in the forested areas than in the nearby non-forested areas (Fig. 6). In the
438 entire ARB, SCD was 12 days shorter in the forested area than in the non-forested areas although
439 most of forested areas are distributed in the northern ARB and in higher elevation zones (Fig. 15a).
440 At the similar climatic settings in the Sanjiang Plain, SCD was 21 days shorter in the forested areas
441 than in the non-forested areas (Fig. 15b). Part of this shorter SCD in the forested areas could be
442 explained by the less estimate of MODIS snow cover mapping algorithm (Xin et al., 2012; Raleigh
443 et al., 2013).

444 The dominant cause is likely due to the less snow accumulation within the forested areas than
445 on the nearby farmland, e.g., in the two case areas of forest and farmland in the Sanjiang Plain (Figs.
446 15b). Depending on specific conditions, up to 60% of cumulative snowfall could be intercepted and
447 sublimated back to atmosphere (Pomeroy, 1998). Snow accumulated in forested areas was up to 40%
448 lower than that in nearby clearing sites (e.g. Winkler et al., 2005; Jost et al., 2007). Meanwhile, the
449 snowmelt rates could be up to 70% lower in forests than in open areas due to the shelter and
450 shading effect of forest on ground snow (e.g. Varhola et al., 2010). The lower snowmelt rate would
451 cause snow persisting about 10 days longer under the forest canopy than in the nearby clearings
452 although there might be less snow accumulation under forest canopy, e.g. in the study sites of Sierra
453 Nevada (Raleigh et al., 2013). There are complex interactions between forest and snow. Whether
454 SCD persists longer or shorter than the nearby clearings is found to be a function of latitude, aspect,
455 forest structure, climate and seasonal meteorology (Molotch et al., 2009; Musselman et al., 2012).

456 **5.2 Snow cover variations**

457 The MODIS snow cover extent showed a slightly increase trend during the 14 snow
458 hydrological years from HY2000 to HY2014 in ARB, primarily consisting of Russia and China (Fig.



459 12). The northern ARB (Russia) had a smaller increase rate than the southern ARB (China), and
460 March and April had a larger increase rate than other months in China (Table 6). Since the forest
461 cover fractions in China, Russia and ARB were 38%, 63% and 47%, respectively, this leads to a
462 larger increase rate in the non-forested area than in the forested area in the entire ARB (Table 7). In
463 contrast, in the similarly climatic conditions at the two nearby areas in the SanJiang Plain (Fig. 1),
464 the forested areas showed much shorter SCD and slightly larger increase rates than in the
465 non-forested area (Table 8).

466 The increase trends of snow cover in ARB is consistent with the study of Chen et al. (2014) that
467 the snow cover extent and precipitation in the northeast China (mostly in the southern ARB)
468 showed an increase trend during the 10 years from HY2004 to HY2013, while air temperature
469 presented a decrease trend. During the snowy season, snow cover extent was negatively correlate
470 with the air temperature (Chen et al., 2014), especially in the melting season of March and April,
471 when the variations of air temperature can explain 74% and 86% of the mean SCF in Russia and
472 China, respectively (Fig. 13). Compare to the reference period from 1961 to 1990, the annual mean
473 air temperature in the periods of 1991-2000 and 2001-2015 increased by 1.0°C and 1.1°C in China
474 and 0.9°C and 1.1°C in Russia, respectively. The air temperature showed a decrease trend since
475 2007 and did not begin to increase until 2014 (Fig. 14), resulting in an increasing SCF from
476 HY2000 to HY2013, especially in HY2012 (Figs. 12 and 15).

477 The change trends of snow cover and air temperature in ARB during the recent 15 years in the
478 21st century are different from the long-term trend from 1950 to 2010, when annual mean air
479 temperature increased significantly by 1.4-2.4°C in different regions, and precipitation only had an
480 increase trend in the ARB downstream region (Yu et al., 2013). According to the in situ snow depth



481 measurements, Li et al. (2009) found that SCOD retreated by 1.9 days per decade and SCED
482 advanced 1.6 days per decade from 1961 to 2005 in the Heilongjiang Province, China, although the
483 cumulative snow depth showed an increase trend (Chen and Li, 2011). The changes of snow cover
484 duration occurred primarily in the plains, while increases of snow depth took place in mountains (Li
485 et al., 2009). The snow changes in ARB were also different from the monthly mean snow cover
486 extent in the North Hemisphere, which decreased about 5% from 1960s to 2000s (Barry et al.,
487 2009). In March and April, the mean snow cover extent in Northern Hemisphere decreased
488 $1.6\% \pm 0.8\%$ per decade in the period from 1967 to 2012 (IPCC, 2013). Although the snow cover
489 extent in ARB demonstrated a different change pattern during the recent 14 years compared to the
490 long-term trend since 1950s in the context of global warming, the increasing air temperature in
491 ARB projects a decrease of snow cover extent and periods in the coming years.

492

493 **6. Conclusions**

494 The study applies the improved cloud-free MODIS daily snow cover product (MODMYD_MC)
495 to investigate the snow cover variations from HY2000 to HY2013 in the Amur River Basin. The
496 fractions of forest cover were 38%, 63% and 47% in 2009 in China (the southern ARB), Russia (the
497 northern ARB) and ARB, respectively. Forest demonstrates complex impacts on the snow
498 accumulation and melting processes and on optical satellite snow cover mapping. Validation results
499 show that MODMYD_MC has a snow agreement of 88% against *in situ* snow depth observations
500 ($\geq 4\text{cm}$). The agreement is about 10% lower at the forested stations than at the non-forested stations
501 although the former mean snow depth is 5 cm larger. SCDs from MODMYD_MC are 20 days
502 shorter than *in situ* observations at the forested stations, while they are closer (-8 days) to those at



503 the non-forested stations. Annual mean SCDs from MODMYD_MC in the forested areas were
504 greatly shorter (-21days) than those in the nearby farmland in the SanJiang Plain.

505 SCD/SCF is negatively correlated with air temperature in ARB, especially in the snow melting
506 season, when the mean air temperature in March and April can explain 86% and 74% of the mean
507 SCF variations in China and Russia, respectively. From 1961 to 2015, the annual mean air
508 temperature presented an increase trend by 0.33°C/decade in both China and Russia, while it had a
509 decrease trend during the study period from HY2000 to HY2013. The decrease of air temperature
510 resulted in an increase of snow cover although the increase of snow cover was not significant above
511 the 90% confidence level. SCD/SCF had larger increase rates in China than in Russia, and they
512 were larger in the forested area than in the nearby farmland in the similarly climatic settings in the
513 SanJiang Plain. The air temperature began to increase again in 2014 and 2015, and the increasing
514 air temperature in ARB projects a decrease of snow cover extent and periods in the coming years.

515 **Acknowledgements:**

516 This study is funded by the Open Foundation of the State Key Laboratory of Desert and Oasis
517 Ecology, Xinjiang Institute of Ecology and Geography, Chinese Academy of Sciences
518 (#G2014-02-06), Natural Science Foundation of China (#41371404), Fundamental Research Funds
519 from Sun Yat-sen University (#15lgzd06), National Basic Research Program of China
520 (#2012CB955903) and the Startup Foundation for Oversea Returnees from the Department of
521 Education of China (#2013693). We thank the US NASA and NSIDC for providing the MODIS
522 land cover and snow cover products and the Heilongjiang Climate Data Center for the *in situ* snow
523 depth data.

524



525 **References:**

- 526 **Barry, R.G.**, Armstrong, R., Callaghan, T., Cherry, J., Nolin, A., and Russell, D. Chapter 4: Snow. *Global*
527 *Outlook for Ice and Snow*, United Nations Environment Programme. ISBN: 978-92-807-2799-9, Job No:
528 DEW/0924/NA, 2009.
- 529 **Brown, R.**, Derksen, C., Wang, L.: Assessment of spring snow cover duration variability over northern Canada
530 from satellite datasets, *Remote Sens. Environ.*, 71, 297–308, 2007.
- 531 **Chapin, F.**, Sturm, M., Serreze, M., McFadden, J., Key, J., Lloyd, A., et al.: Role of land-surface
532 changes in Arctic summer warming, *Science*, 310, 657–660m, 2005.
- 533 **Chen, G. and Li, D.**: Temporal-spatial characteristics of cumulative snow depth in Northeast China
534 and its vicinity, *Meteorological Monthly*, 37(5), 513-521, 2011 (In Chinese).
- 535 **Chen, S.**, Yang, Q., Xie, H., Zhang, H., Lu, P. and Zhou, C.: Spatiotemporal variations of snow
536 cover in northeast China based on flexible multiday combinations of moderate resolution
537 imaging spectroradiometer snow cover products, *Journal of Applied Remote Sensing*, Vol.8,
538 084685-15,2014..
- 539 **Dale, V.H.** and Polasky, S.: Measures of the effects of agricultural practices on ecosystem services,
540 *Ecol. Econ.*, 64, 286–296, 2007.
- 541 **Dickerson-Lange, S. E.**, Lutz, J.A., Martin, K.A., Raleigh, M.S., Gersonde, R. and Lundquist, J.D.:
542 Evaluating observational methods to quantify snow duration under diverse forest canopies,
543 *Water Resour. Res.*, 51, doi: 10.1002/2014WR015744, 2015.
- 544 **Friedl, M.A.**, Sulla-Menashe, D., Tan, B., Schneider, A., Ramankutty, N., Sibley, A. and Huang, X.:
545 MODIS Collection 5 global land cover: Algorithm refinements and characterization of new
546 datasets, *Remote Sensing of Environment*, 114, 168–182, 2010.



- 547 **Gao, Y.**, Xie, H., Yao, T. and Xue, C.: Integrated assessment on multi-temporal and multi-sensor
548 combinations for reducing cloud obscuration of MODIS snow cover products of the Pacific
549 Northwest USA, *Remote Sensing of Environment*, 114, 1662-1675, 2010.
- 550 **Golding, D.** and Swanson, R.: Snow distribution patterns in clearings and adjacent forest, *Water*
551 *Resour. Res.*, 22 (13), 1931–1940, 1986.
- 552 **Hall, D.K.**, Riggs, G.A. and Salomonson, V.V.: Development of methods for mapping global snow
553 cover using moderate resolution imaging spectroradiometer data, *Remote Sensing of*
554 *Environment*, 54, 127–140, 1995.
- 555 **Hall, D.K.**, Riggs, G.A., Salomonson, V.V., DiGirolamo, N.E., Bayr, K.J. 2002. MODIS
556 snow-cover products. *Remote sensing of Environment*, 83, 181-194.
- 557 **Hall, D.K.**, Riggs, G.A., Foster, J.L. and Kumar, S.V.: Development and evaluation of a
558 cloud-gap-filled MODIS daily snow-cover product, *Remote Sensing of Environment*, 114,
559 496-503, 2010..
- 560 **IPCC**: Summary for Policymakers. In: Climate Change 2013: The Physical Science Basis.
561 Contribution of Working Group I to the Fifth Assessment Report of the Intergovernmental
562 Panel on Climate Change [Stocker, T.F., D. Qin, G.-K. Plattner, M. Tignor, S. K. Allen, J.
563 Boschung, A. Nauels, Y. Xia, V. Bex and P.M. Midgley (eds.)]. Cambridge University Press,
564 Cambridge, United Kingdom and New York, NY, USA, 2013.
- 565 **Jost, G.**, Weiler, M., Gluns, D. and Alila, Y.: The influence of forest and topography on snow
566 accumulation and melt at the watershed-scale, *J. Hydrol.*, 347, 101-115, 2007.
- 567 **Klein, A.G.**, Hall, D.K. and Riggs, G.A.: Improving snow cover mapping in forests through the use
568 of a canopy reflectance model, *Hydrological Processes*, 12, 1723–1744, 1998.
- 569 **Lei, X.**, Song, K., Wang, Z., Zhong, G., Zhao, K., Liu, D. and Zhang, B.: Accuracy evaluation of



- 570 MODIS and AMSR-E snow cover products in the Heilongjiang drainage basin, *Journal of the*
571 *Graduate School of the Chinese Academy of Sciences*, 28, 43-50, 2011 (In Chinese).
- 572 **Liang, T.**, Zhang, X., Xie, H., Wu, C., Feng, Q., Huang, X. and Chen, Q.: Toward improved daily
573 snow cover mapping with advanced combination of MODIS and AMSR-E measurements,
574 *Remote Sensing of Environment*, 112, 3750-3761, 2008.
- 575 **Li, F.**, Zhang, B. and Zhang, S.: Ecosystem service valuation of Sanjiang Plain, *Journal of Arid*
576 *Land Resources and Environment*, 18(5), 19-24, 2004 (In Chinese).
- 577 **Li, D.**, Liu, Y., Yu, H. and Li, Y.: Spatial-Temporal Variation of the Snow Cover in Heilongjiang
578 Province in 1951 -2006, *Journal of Glaciology and Geocryology*, 31 (6), 1011-1018, 2009. (In
579 Chinese)
- 580 **Liu, J.**, Melloh, R.A., Woodcock, C.E., Davis, R.E., Painter, T.H. and McKenzie, C.: Modeling the
581 view angle dependence of gap fractions in forest canopies: implications for mapping fractional
582 snow cover using optical remote sensing, *Journal of Hydrometeorology*, 9, 1005–1019, 2008.
- 583 **Moeser, D.**, Mazzotti, G., Helbig, N. and Jonas, T.: Representing spatial variability of forest snow:
584 Implementation of a new interception model, *Water Resour. Res.*, 52, doi:
585 10.1002/2015WR017961, 2016.
- 586 **Molotch, N.P.**, Brooks, P.D., Burns, S.P., Litvak, M., Monson, R.K., McConnell, J.R. and
587 Musselman, K.N.: Ecohydrological controls on snowmelt partitioning in mixed-conifer
588 sub-alpine forests, *Ecohydrology*, 2 (2), 129–142, 2009.
- 589 **Musselman, K.N.**, Molotch, N.P., Margulis, S.A., Kirchner, P.B. and Bales, R.C.: Influence of
590 canopy structure and direct beam solar irradiance on snowmelt rates in a mixed conifer forest,
591 *Agricultural and Forest Meteorology*, 161, 46 - 56. [http://dx.doi.org](http://dx.doi.org/10.1016/j.agrformet.2012.03.011)
592 [/10.1016/j.agrformet.2012.03.011](http://dx.doi.org/10.1016/j.agrformet.2012.03.011), 2012.



- 593 **Ott, R. L.**, Larson, R., Rexroat, C. and Mendenhall, W.: Statistics: a Tool for the Social Sciences,
594 PWS-Kent Publishing Company, Boston, MA, USA, 1992.
- 595 **Parajka, J.** and Blöschl, G.: Spatio-temporal combination of MODIS images–potential for snow
596 cover mapping, *Water Resources Research*, 44, W3406, 2008.
- 597 **Parajka, J.**, Pepe, M., Rampini, A., Rossi, S. and Blöschl, G.: A regional snow-line method for
598 estimating snow cover from MODIS during cloud cover, *Journal of Hydrology*, 381, 203-212,
599 2010.
- 600 **Paudel, K.P.** and Andersen, P.: Monitoring snow cover variability in an agropastoral area in the
601 Trans Himalayan region of Nepal using MODIS data with improved cloud removal
602 methodology, *Remote Sensing of Environment*, 115, 1234-1246, 2011.
- 603 **Pomeroy, J.W.**, Parviainen, J., Hedstrom, N. and Gray, D.M.: Coupled modelling of forest snow
604 interception and sublimation, *Hydrol. Proc.*, 12, 2317–2337, 1998.
- 605 **Raleigh, M.S.**, Rittger, K., Moore, C.E., Henn, B., Lutz, J.A. and Lundquist, J.D.: Ground-based
606 testing of MODIS fractional snow cover in subalpine meadows and forests of the Sierra Nevada,
607 *Remote Sens. Environ.*, 128, 44–57, 2013.
- 608 **Robinson, D.**: Northern Hemisphere continental snow cover extent: 2014 update. Rutgers
609 University, Retrieved on September 15, 2015 at website: <http://climate.rutgers.edu/snowcover>,
610 2015.
- 611 **Varhola, A.**, Coops, N.C., Weiler, M. and Moore, R.D.: Forest canopy effects on snow
612 accumulation and ablation: An integrative review of empirical results, *J. Hydrol.*, 392(3-4),
613 219–233, 2010.
- 614 **Wang, Z.**, Zhang, B., Zhang, S., Li, X., Liu, D., Song, K., Li, J., Li, F. and Duan, H.: Changes of
615 land use and of ecosystem service values in Sanjiang Plain, Northeast China, *Environ Monit*



- 616 *Assess*, 112, 69–91, 2006.
- 617 **Wang, X.**, Xie, H. and Liang, T.: Evaluation of MODIS snow cover and cloud mask and its
618 application in Northern Xinjiang, China, *Remote Sensing of Environment*, 112, 1497-1513,
619 2008.
- 620 **Wang, J.**, Lu, X., Jiang, M., Li, X. and Tian, J.: Synthetic evaluation of wetland soil quality
621 degradation: A case study on the Sanjiang Plain, Northeast China, *Pedosphere*, 19:756–64,
622 2009a.
- 623 **Wang, X.**, Xie, H., Liang, T. and Huang, X.: Comparison and validation of MODIS standard and
624 new combination of Terra and Aqua snow cover products in northern Xinjiang, China,
625 *Hydrological Processes*, 23, 419-429, 2009b.
- 626 **Wang, X.** and Xie, H.: New methods for studying the spatiotemporal variation of snow cover based
627 on combination products of MODIS Terra and Aqua. *Journal of hydrology*, 371, 192-200,
628 2009.
- 629 **Wang, X.**, Zheng, H., Chen, Y., Liu, H., Liu, L., Huang, H. and Liu, K.: Mapping snow cover
630 variations using a MODIS daily cloud-free snow cover product in Northeast China, *Journal of*
631 *Applied Remote Sensing*, 8(1), 084681. doi:10.1117/1.JRS.8.084681, 2014.
- 632 **Wang, Z.**, Mao, D., Li, L., Jia, M., Dong, Z., Miao, Z., Ren, C. and Song, C.: Quantifying changes
633 in multiple ecosystem services during 1992-2012 in the Sanjiang Plain of China, *Science of the*
634 *Total Environment*, 514, 119-130, 2015.
- 635 **Winkler, R.D.**, Spittlehouse, D.L. and Golding, D.L.: Measured differences in snow accumulation
636 and melt among clearcut, juvenile, and mature forests in southern British Columbia, *Hydrol.*
637 *Proc.*, 19, 51–62, 2005.
- 638 **Xie, H.**, Wang, X. and Liang, T.: Development and assessment of combined Terra and Aqua snow



- 639 cover products in Colorado Plateau, USA and northern Xinjiang, China, *Journal of Applied*
640 *Remote Sensing*, 3, 1-14, 2009.
- 641 **Xin**, Q., Woodcock, C.E., Liu, J., Tan, B., Melloh, R.A. and Davis, R.E.: View angle effects on
642 MODIS snow mapping in forests, *Remote Sensing of Environment*, 118, 50-59, 2012.
- 643 **Xu**, Y.M., Li, Y., Ouyanga, W., Hao, F.H., Ding, Z.L. and Wang, D.L.: The impact of long-term
644 agricultural development on the wetlands landscape pattern in Sanjiang Plain, *Procedia*
645 *Environmental Sciences*, 13 (2012), 1922-1932, 2012.
- 646 **Yang**, D., Robinson, D., Zhao, Y., Estilow, T. and Ye, H.: Streamflow response to seasonal snow
647 cover extent changes in large Siberian watersheds, *Journal of Geophysical Research*, 108(D18),
648 4578-4591, 2003.
- 649 **Yu**, L.L., Xia, Z.Q., Li, J.K. and Cai, T.: Climate change characteristics of Amur River, *Water*
650 *Science and Engineering*, 6(2): 131-144, 2013.
- 651 **Zhang, H.:** Study on Spatio-temporal Variations of Snow from 2000 to 2009 in Northeast China.
652 *Master Thesis*. Jilin University, 2010. (In Chinese)
653



654 Table 1. Summary of snow and snow-free land recorded by ground measurements and MODMYD_MC retrievals
 655 for ten years from 2000 to 2010 at four typical stations representing cultivated farmland, natural grassland and
 656 forests. The number in the parenthesis is percentage.

Stations	Land cover/use	Elevation (m)	Latitude (degree)	Longitude (degree)	Days (SD \geq 1cm)	Snow from MODIS	Days (SD \geq 4cm)	Snow from MODIS
Suiling, S31	Farmland	202	47.14	127.06	1136	1058 (93%)	857	839 (98%)
Jiamusi, S53	Grassland	81	46.49	130.17	1213	1128 (93%)	1026	991 (97%)
Yichun, S12	Forest	240	47.44	128.55	1302	806 (88%)	1093	751 (92%)
Yilan, S52	Forest	100	46.15	129.350	1047	597 (57%)	644	444 (69%)

657
 658

659 Table 2. The snow cover fraction in different pixel patches centered at stations S31 (cultivated farmland) in snow
 660 hydrologic years of 2007/9/1-2008/8/31 (HY2007) with least snow and 2009/9/1-2010/8/31 (HY2009) with most
 661 snow.

Snow depth (cm)	Hydrologic Year	Ground SCD	Snow cover fraction from MODMYD_MC at S31				
			1 \times 1	3 \times 3	5 \times 5	9 \times 9	21 \times 21
SD=0	HY2007	280	1%	1%	1%	1%	1%
	HY2009	217	1%	1%	1%	1%	1%
1 \leq SD \leq 3	HY2007	36	72%	77% [/]	75%	73%	74%
	HY2009	11	82%	76%	77%	77%	79%
SD \geq 4	HY2007	49	97%	98%	97%	97%	98%
	HY2009	137	100%	100%	100%	100%	100%
Max Snow Depth = 13cm on Dec 31, 2007			100%	100%	100%	95%	97%
Max Snow Depth = 26cm on Mar 16, 2010			100%	100%	100%	100%	100%
Forest Fraction from MCD12Q1 in 2009			0%	0%	0%	0%	0%

662
 663 +



664 Table 3. The snow cover fraction in different pixel patches centered at stations S53 (grassland) in snow hydrologic
 665 years of 2007/9/1-2008/8/31 (HY2007) with least snow and 2009/9/1-2010/8/31 (HY2009) with most snow.

Snow depth (cm)	Hydrologic Year	Ground SCD	Snow cover fraction from MODMYD_MC at S53				
			1×1	3×3	5×5	9×9	21×21
SD=0	HY2007	296	3%	1%	1%	2%	3%
	HY2009	218	3%	2%	2%	3%	3%
1≤SD≤3	HY2007	4	25%	18%	45%	14%	12%
	HY2009	5	60%	45%	19%	39%	41%
SD≥4	HY2007	65	94%	96%	92%	88%	89%
	HY2009	142	95%	95%	95%	91%	92%
Max Snow Depth = 32cm on Dec 31, 2007			100%	100%	100%	96%	96%
Max Snow Depth = 42cm on Mar 16, 2010			100%	100%	100%	98%	99%
Forest Fraction from MCD12Q1 in 2009			0%	0%	23%	13%	15%

666
 667

668 Table 4. The snow cover fraction in different pixel patches centered at stations S12 (forest) in snow hydrologic
 669 years of 2007/9/1-2008/8/31 (HY2007) with least snow and 2009/9/1-2010/8/31 (HY2009) with most snow

Snow depth (cm)	Hydrologic Year	Ground SCD	Snow cover fraction from MODMYD_MC at S12				
			1×1	3×3	5×5	9×9	21×21
SD=0	HY2007	256	3%	2%	1%	2%	4%
	HY2009	202	3%	1%	3%	2%	3%
1≤SD≤3	HY2007	39	51%	63%	58%	58%	55%
	HY2009	8	88%	85%	87%	86%	86%
SD≥4	HY2007	55	87%	86%	82%	80%	78%
	HY2009	140	87%	88%	87%	87%	85%
Max Snow Depth = 14cm on Dec 31, 2007			100%	65%	51%	46%	39%
Max Snow Depth = 39cm on Mar 16, 2010			100%	100%	100%	100%	99%
Forest Fraction from MCD12Q1 in 2009			100%	100%	100%	100%	100%

670
 671
 672
 673



674 Table 5. The snow cover fraction in different pixel patches centered at stations S52 (forest) in snow hydrologic
 675 years of 2007/9/1-2008/8/31 (HY2007) with least snow and 2009/9/1-2010/8/31 (HY2009) with most snow.

Snow depth (cm)	Hydrologic Year	Ground SCD	Snow cover fraction from MODMYD_MC at S52				
			1×1	3×3	5×5	9×9	21×21
SD = 0	HY2007	292	1%	1%	2%	2%	2%
	HY2009	207	0%	2%	2%	2%	2%
1≤SD≤3	HY2007	29	0%	18%	24%	31%	46%
	HY2009	18	0%	14%	22%	26%	39%
SD ≥ 4	HY2007	44	2%	34%	40%	57%	75%
	HY2009	140	59%	62%	64%	76%	88%
Max Snow Depth = 17cm on Dec 31, 2007			0%	20%	30%	48%	69%
Max Snow Depth = 21cm on Mar 16, 2010			100%	77%	73%	88%	97%
Forest Fraction from MCD12Q1 in 2009			100%	100%	100%	85%	70%

676

677

678 Table 6. The linear trend/slope (s), interception (b) and correlation coefficients (r) of the mean Snow Cover
 679 Fraction (SCF) with time (year) from HY2000 to HY2013 in the Amur River Basin (ARB), Russia and China for
 680 Fig 12b. The r threshold for statistical significance is 0.45 at the 90% confidence levels for n=14 (Ott et al., 1992).

	r			s (percent/year)			b (Percent)		
	ARB	Russia	China	ARB	Russia	China	ARB	Russia	China
Annual	0.27	0.25	0.34	0.30%	0.26%	0.46%	29.60%	35.30%	22.30%
Mar-Apr	0.18	0.09	0.32	0.56%	0.28%	1.10%	42.30%	59.10%	25.50%
Mar	0.22	0.11	0.36	0.78%	0.30%	1.67%	61.10%	77.70%	41.30%

681

682



683 Table 7. The linear trend/slope (s), interception (b) and correlation coefficients (r) of snow cover duration (SCD),
 684 Snow Cover Onset Dates (SCOD) and Snow Cover End Dates (SCED) with time (year) from HY2000 to HY2013
 685 in the forested and non-forested areas in ARB for Fig 15a. The r threshold for statistical significance is 0.45 at the
 686 90% confidence levels for n=14 (Ott et al., 1992). The negative r (smaller) values for SCOD mean that snow
 687 cover starts earlier.

	Forested Areas			Non Forested Areas		
	SCD	SCOD	SCED	SCD	SCOD	SCED
Mean (day)	115	329	79	127	325	87
r	0.23	-0.23	0.20	0.35	-0.50	0.19
s (day/year)	0.97	-0.47	0.50	1.31	-0.75	0.43
b (Julian day)	108	332	75	118	331	83

688

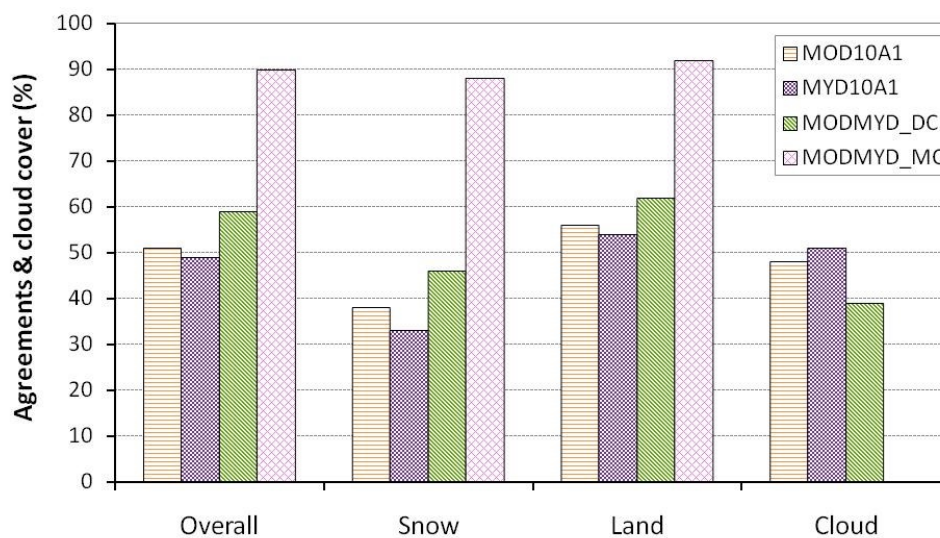
689 Table 8. The linear trend/slope (s), interception (b) and correlation coefficients (r) of snow cover duration (SCD),
 690 Snow Cover Onset Dates (SCOD) and Snow Cover End Dates (SCED) with time (year) from HY2000 to HY2013
 691 in the forested and non-forested areas in the Sanjiang Plain, China for Fig 15b. The r threshold for statistical
 692 significance is 0.45 at the 90% confidence levels for n=14 (Ott et al., 1992). The negative r (smaller) values for
 693 SCOD mean that snow cover starts earlier.

	Forested Areas			Non Forested Areas		
	SCD	SCOD	SCED	SCD	SCOD	SCED
Mean (day)	99	344	78	120	330	84
r	0.39	-0.35	0.33	0.26	-0.13	0.31
s (day/year)	1.61	-0.70	0.91	1.36	-0.47	0.90
b (Julian day)	86	334	70	109	350	77

694

695

696



701

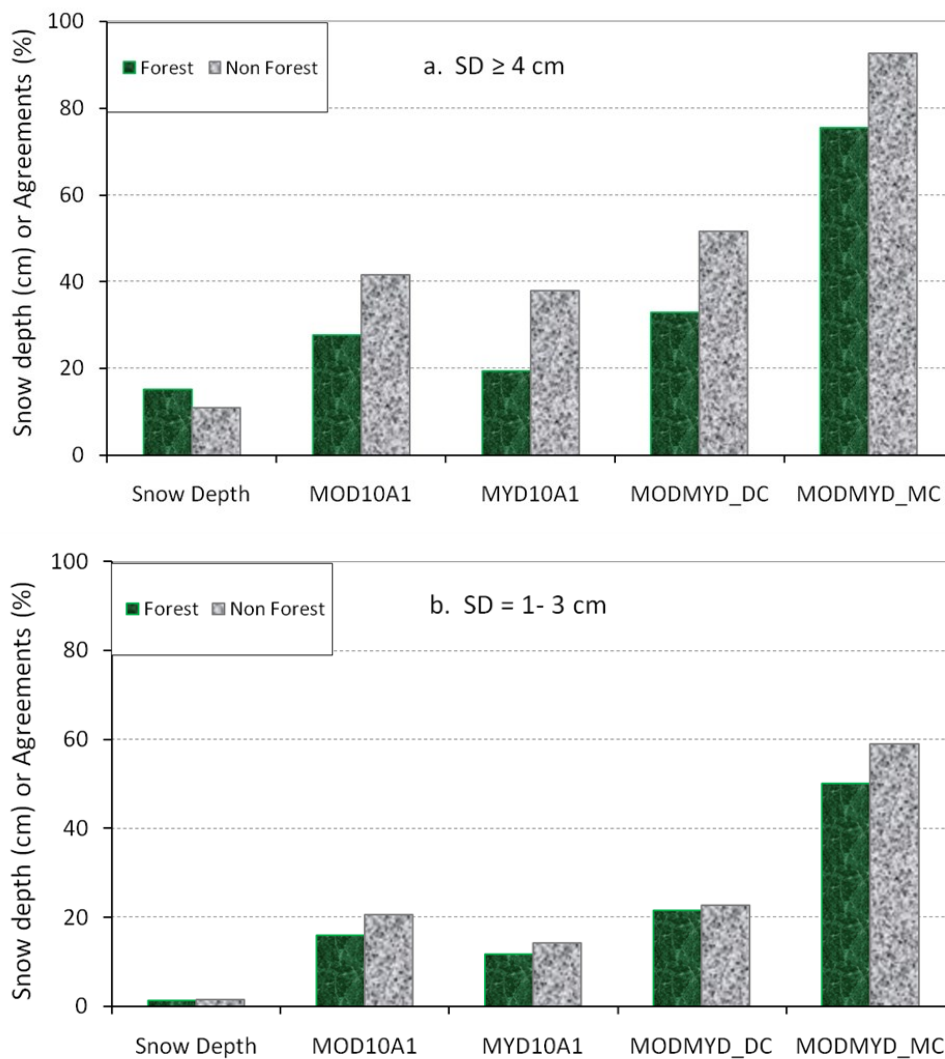
702 Figure 2. The mean agreement of four snow cover products (MOD10A1, MYD10A1,

703 MODMYD_DC, MODMYD_MC) and their cloud fraction (the cloud fraction of MODMYD_MC

704 = 0). On the horizontal X axis, “Snow” and “Land” refer to the agreement (%) of snow or land

705 classifications from MODIS images with the *in situ* measurements of snow depth ≥ 4 cm.

706



707

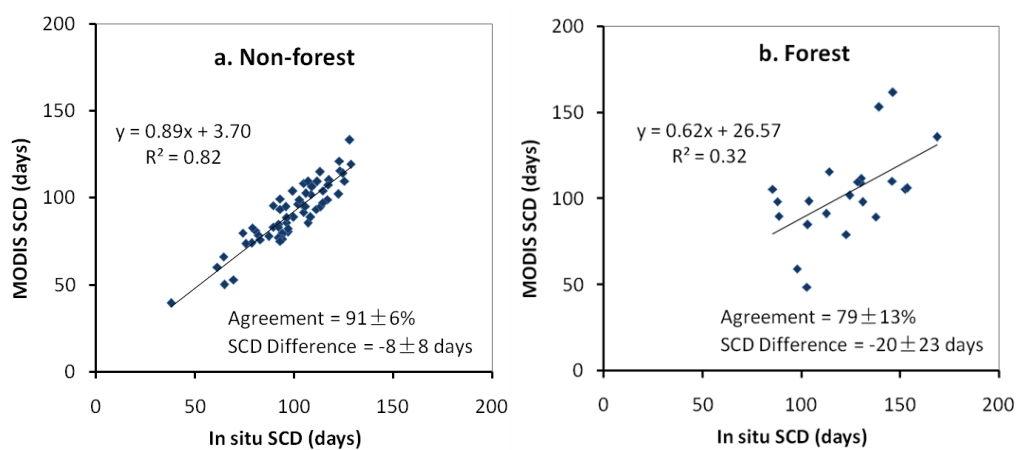
708 Figure 3. The mean agreements of snow cover classifications for the four snow cover products at 57

709 non-forested and 22 forested stations: (a) snow depth \geq 4 cm, (b) snow depth =1-3 cm.

710



711



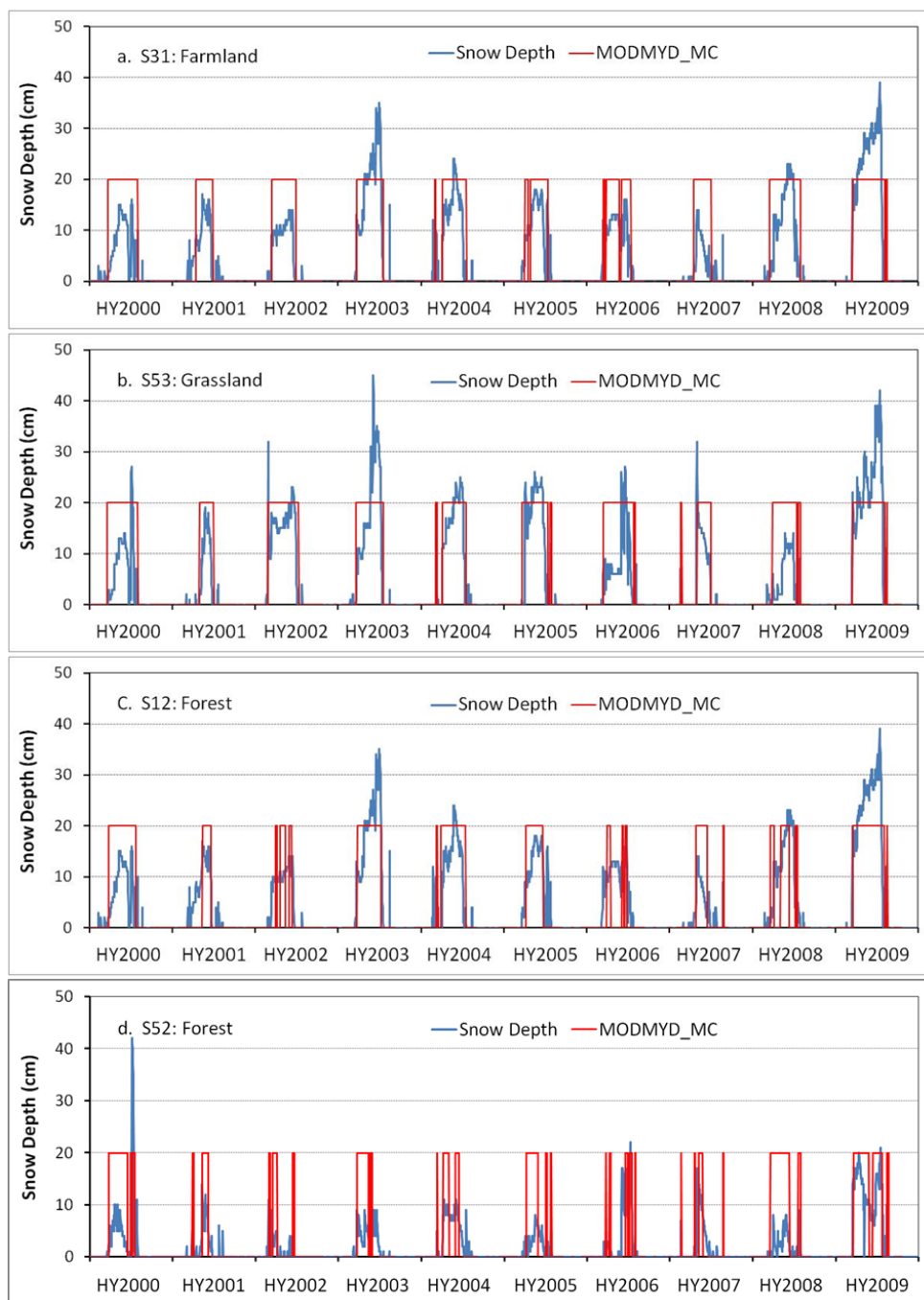
712

713 Figure 4. Comparison of mean snow-covered duration (SCD) from HY2000 to HY2010 between

714 MODMYD_MC and *in situ* observations for all data with snow depth > 0 cm at 57 non-forested

715 stations (a) and 22 forested stations (b).

716



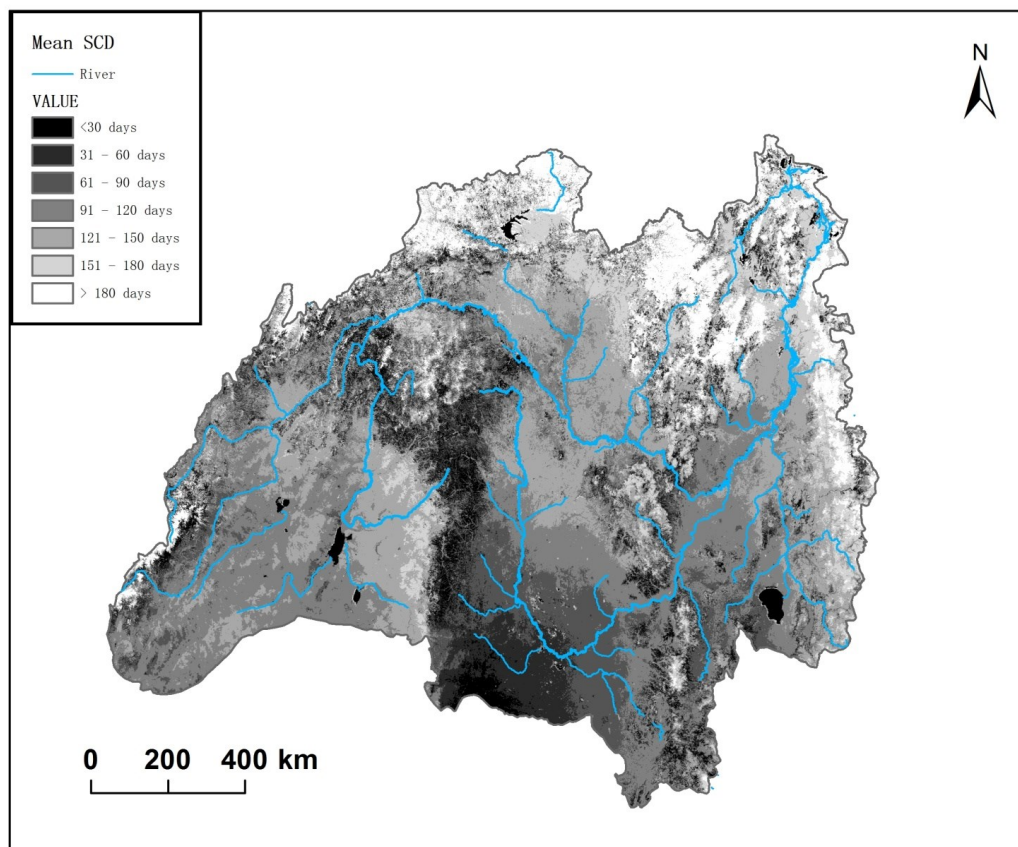
717

718

719

720

Figure 5. Snow depth and MODMYD_MC retrievals at stations of cultivated farmland (S31), natural grassland (S53) and forest (S12 and S52). MODMYD_MC retrievals are shown as 20 cm for snow and 0 for no snow.

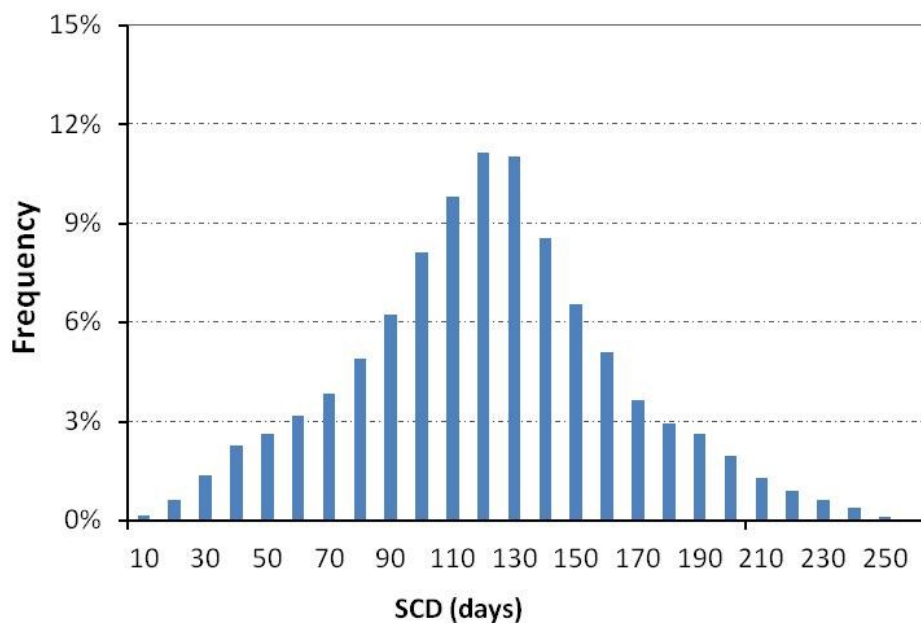


721

722 Figure 6. The spatial distribution of mean snow covered days (SCD) derived from MODMYD_MC from HY2001

723 to HY2014 in the Amur River Basin.

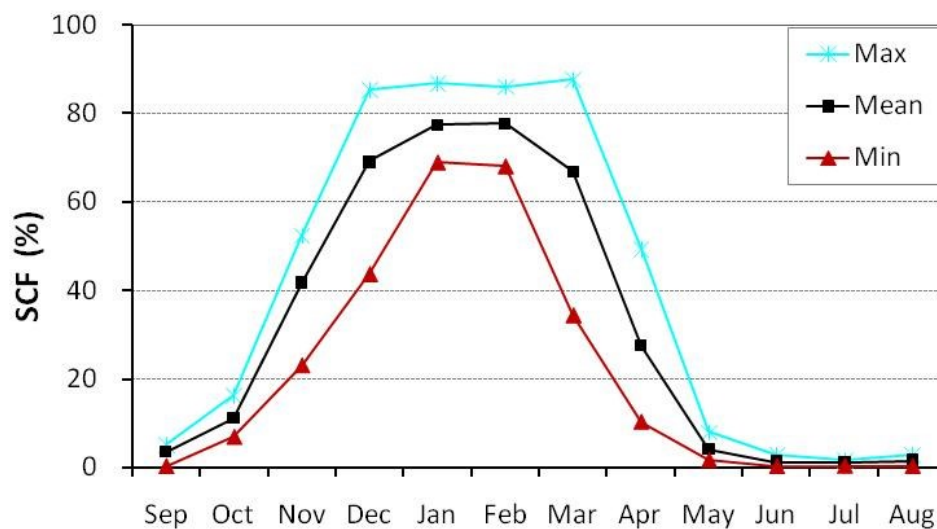
724



725

726 **Figure 7.** The histogram of mean snow-covered days (SCD) computed at a 10-day interval from MODMYD_MC

727 during the period from HY2000 to HY2013.

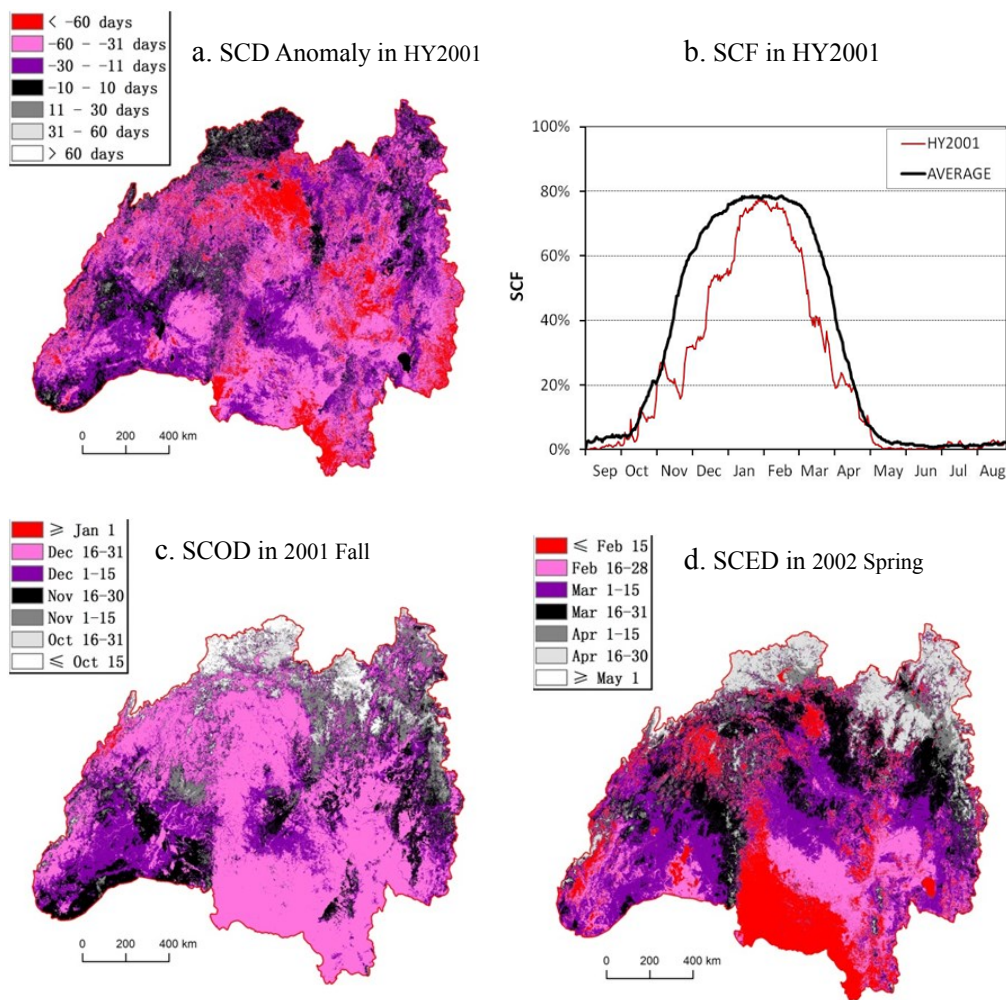


728

729 Figure 8. The minimum, mean and maximum monthly snow cover fraction (SCF) during the period from HY2000
730 to HY2013 computed from MODMYD_MC in the entire Amur River Basin.

731

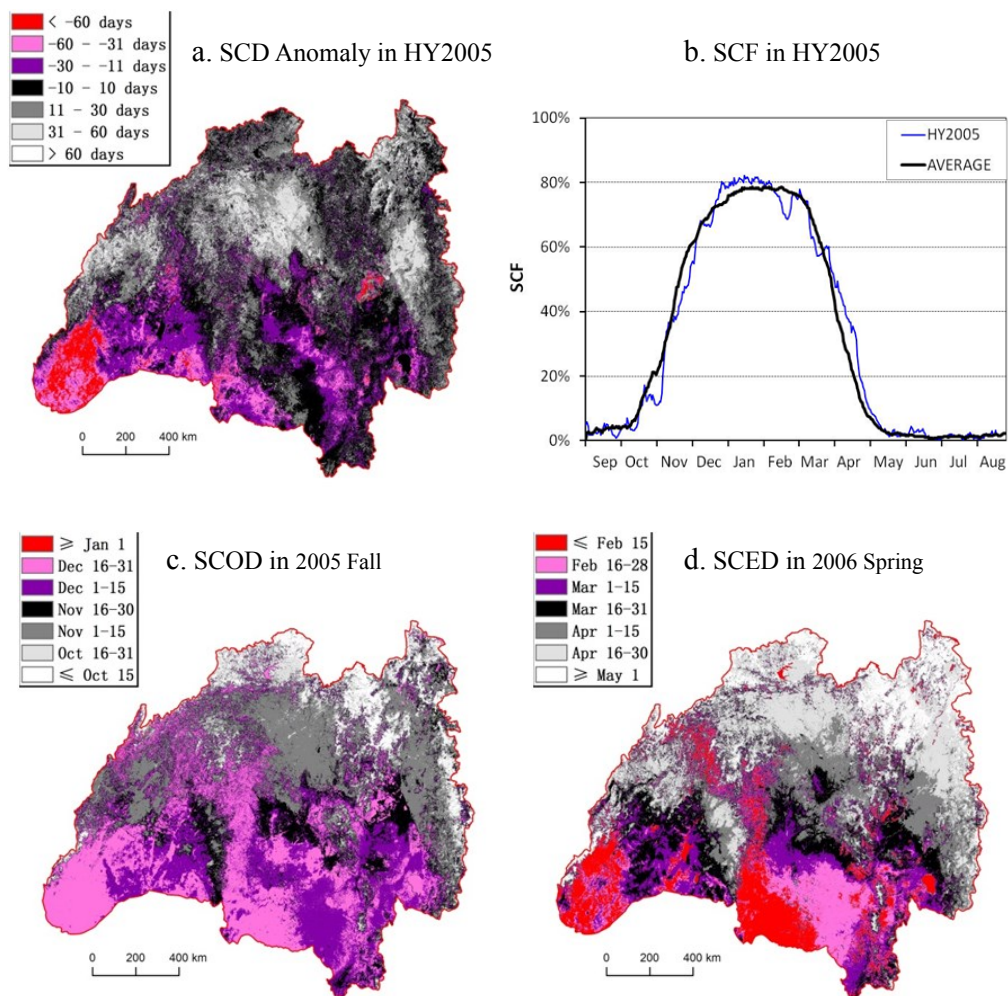
732



733

734 Figure 9. SCD anomaly (a), monthly mean SCF (b), SCOD (c) and SCED (d) in the snow-poor year of HY2001.

735



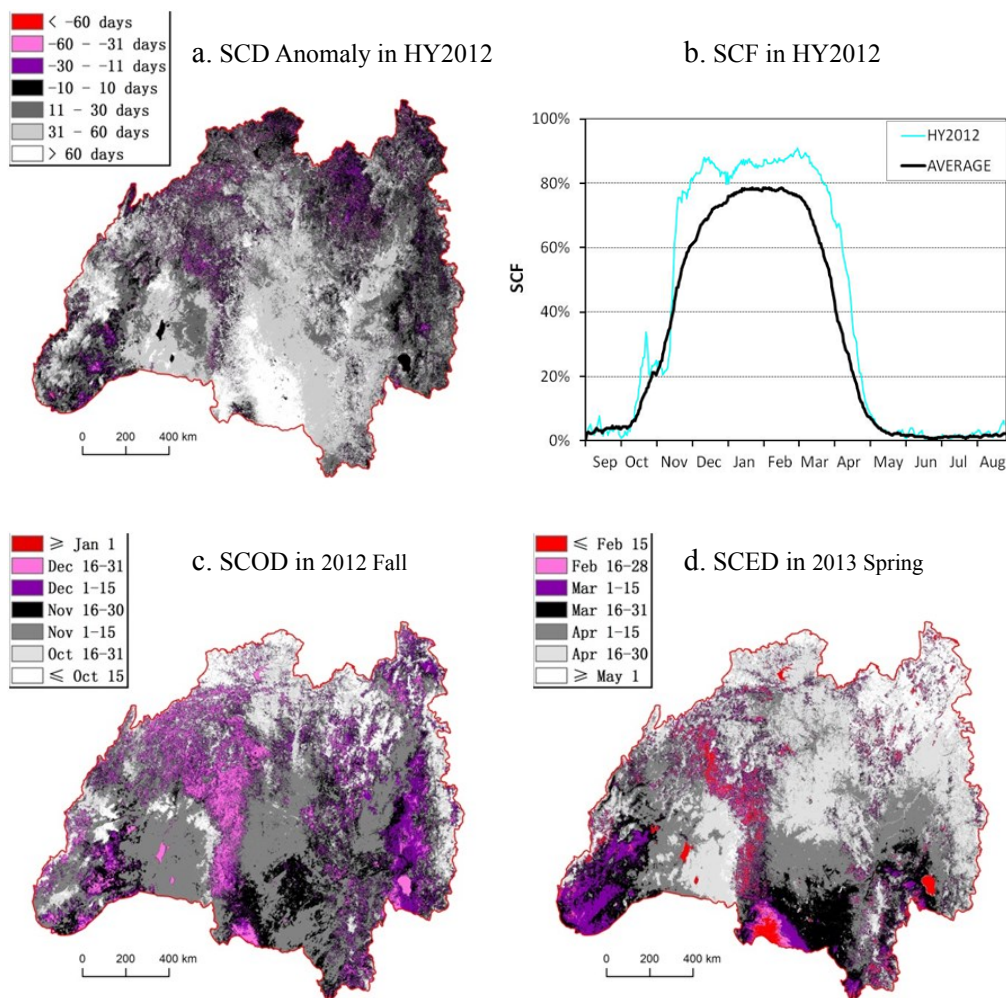
736

737 Figure 10. SCD anomaly (a), monthly mean SCF (b), SCOD (c) and SCED (d) in the snow-neutral year of

738 HY2005.

739

740



741

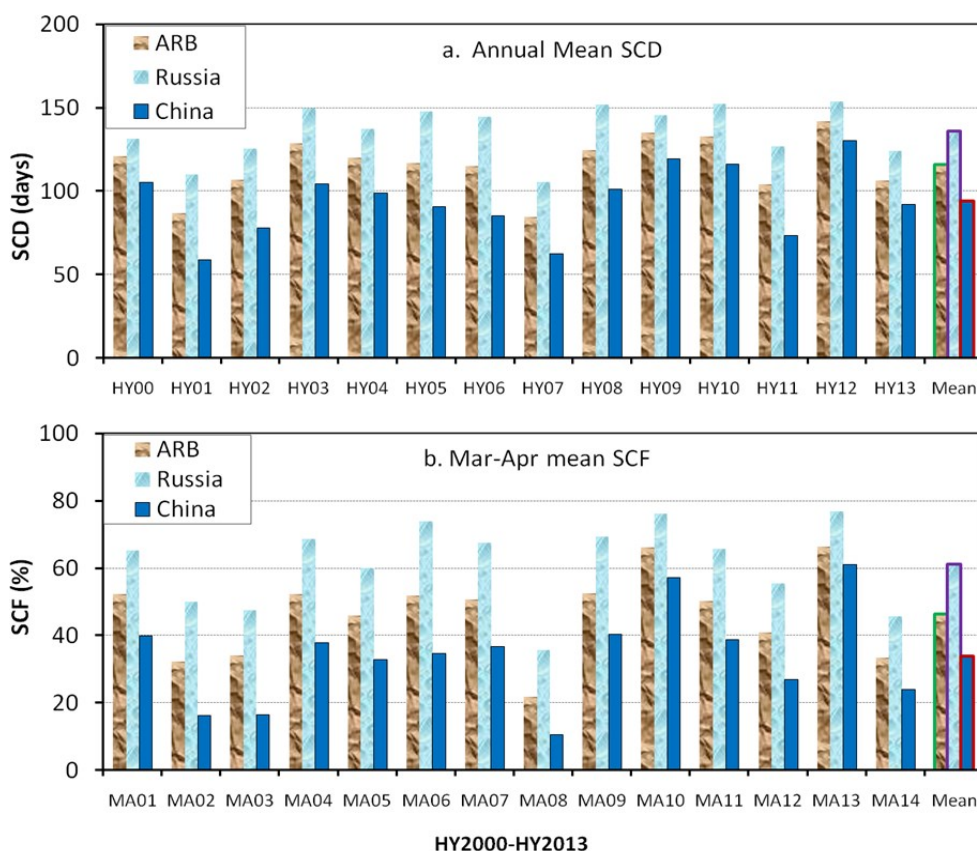
742 Figure 11. SCD anomaly (a), monthly mean SCF (b), SCOD (c) and SCED (d) in the snow-rich year of HY2012.

743

744

745

746



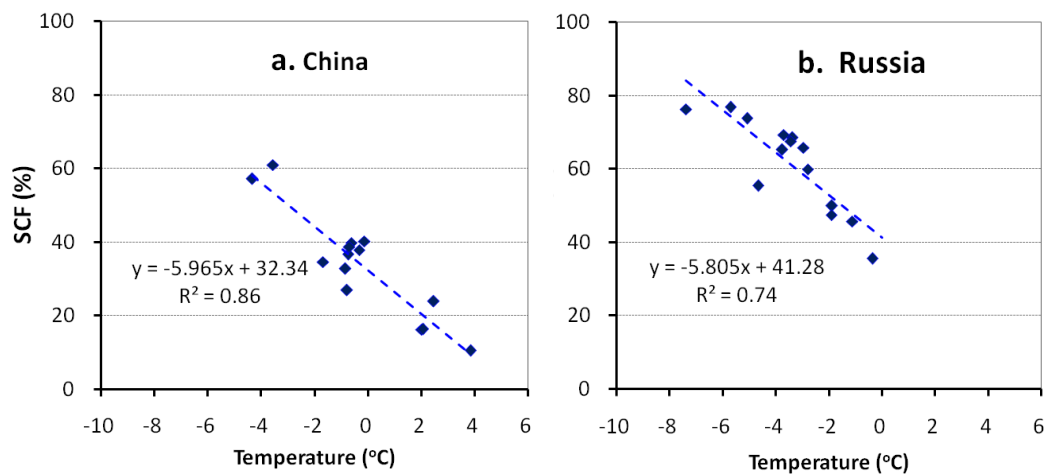
HY2000-HY2013

747
 748

749 Figure 12. The annual snow-covered days (a) and mean snow cover fraction (b) during March and April computed
 750 from MODMYD_MC in the Amur River Basin (ARB), Russia and China from HY2000 to HY2013. MA13 refers
 751 to March and April of 2013, while being in HY2012. The change rates of SCF are summarized in Table 6.

752

753



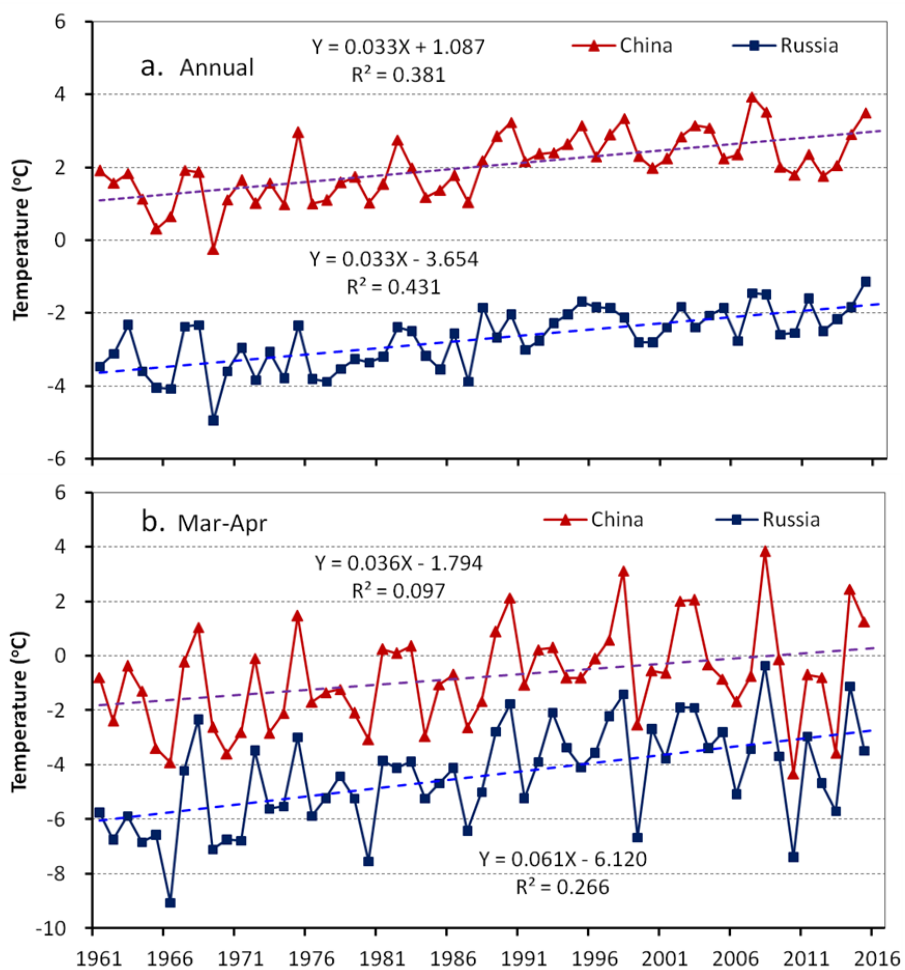
754

755 Figure 13. Scatter plots of mean Snow Cover Fraction (SCF) and air temperature in March and April from 2001 to

756 2014 in China (a) and Russia (b).

757

758

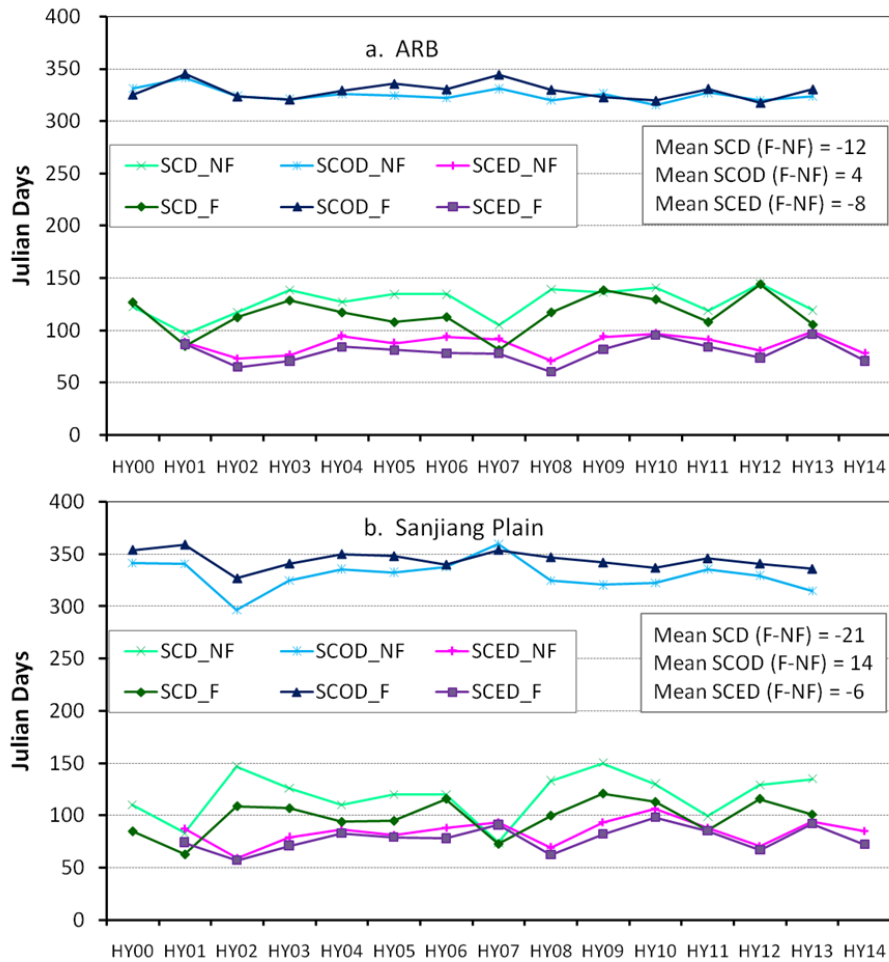


759

760 Figure 14. Annual (a) and Mar-April (b) mean air temperature in China and Russia from 1961 to 2015.

761

762



763

764 Figure 15. The mean snow-covered days (SCD), snow cover onset dates (SCOD) and snow cover end date (SCED)

765 in the forested (F) and non-forested (NF) areas in the entire Amur River Basin and in the Sanjiang Plain from

766 HY2000 to HY2013. The change rates are summarized in Tables 7 and 8.

767

768